INJ INTERNATIONAL NEUROUROLOGY JOURNAL

Feature Fusion Based Ensemble Method For Multi-Level Lung Diseases Classification Of X-Ray Images Using Deep Learning

***J. Jude Moses Anto Devakanth[1], D. Arul Suresh[2], Dr. R. Balasubramanian[3]**

[1,2]Research Scholar, Department of Computer Science and Engineering, Manonmaniam Sundaranar University, Tirunelveli, TamilNadu.

[3]Professor, Department of Computer Science and Engineering, Manonmaniam Sundaranar University, Tirunelveli, TamilNadu.

Abstract

In recent years, infectious respiratory illnesses have surpassed all other causes of death in the world. Pneumonia, Tuberculosis (TB) and COVID-19 are the most severe and prevalent infectious respiratory disorders caused by bacteria and virus that typically affect the lungs which can even lead to death. Currently, COVID-19 is ranked as the highest cause of death in recent years as the mortality rate crosses 6 million. The most interesting and complicating fact about these respiratory diseases are the similarity in their symptoms. So, it is necessary to classify all the three diseases which can be accomplished by applying deep learning techniques in Chest X Ray (CXR) images of patients. Deep learning based multi-level classification is carried out in this research to detect whether the patient is affected by Pneumonia or Tuberculosis or COVID-19. Features plays a major role in classification and so it is decided to develop a novel feature extraction technique namely "Fusion of Handcrafted and Deep features" (FHD). The proposed FHD technique generates a new ensemble Feature Vector (FV) by concatenating handcrafted and deep features and it achieves a classification accuracy of 96.2% using ensemble FV. Handcrafted features include texture features obtained from Gray-level co-occurrence matrix (GLCM), Grey Level Difference Matrix (GLDM) and Gray Level Size Zone Matrix (GLSZM). Extraction of deep features and classification is done by Modified XceptionNet. The results obtained using the proposed technique is reliable and effective, hence radiologists can utilize this method to detect lung disorders using CXR images.

Key words: Feature Extraction, Deep learning, Pneumonia, Tuberculosis, COVID-19 classification.

Introduction

Due to the increased prevalence and effective impact of various diseases, healthcare is now become the primary concern in people's daily lives as never before. Nowadays, millions of humans are affected and killed by numerous respiratory disorders like COVID-19, pneumonia, and tuberculosis (TB) each year. The ratio is anticipated to increase annually [1,56]. The global healthcare system has come under a lot of pressure as a result of the terrible pandemic known as COVID-19 and its exponentially increasing number of cases. It is also stated that more people died of various respiratory illnesses than COVID-19 during the pandemic. Prior to COVID-19, tuberculosis was the most fatal infectious disease, with a pronounced annual increase in the number of deaths. Another respiratory illness that can be fatal is pneumonia, which is also a severe type of pulmonary tuberculosis. Therefore, it is observed that Pneumonia and tuberculosis (TB) are similar deadly illnesses like COVID-19 [26,53]. As a result, rapid and accurate diagnosis of these diseases is necessary for giving effective treatment and preserving lives [4,27]. The mortality rate of Pneumonia [22], TB [24] and COVID-19 [21] in 2020 and the mortality rate of COVID-19 from 2021 to 2023 is collected from World Health Organization (WHO) and shown in Figure 1.

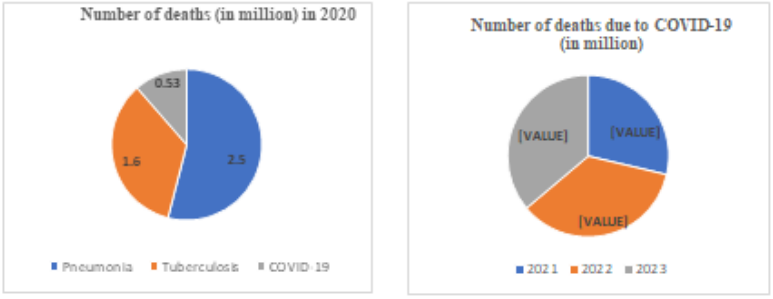

Figure 1. Mortality rates of Pneumonia, Tuberculosis and COVID-19

Medical image processing plays a noteworthy role in diagnosing various diseases [43]. In order to make a proper diagnosis, each disease must be precisely identified through the integration of methodologies and techniques that promote more efficient clinical diagnosis based on pictures generated by various imaging modalities, which are being used more frequently and successfully to diagnose illnesses [35]. Different forms of medical images are available namely Magnetic Resonance Imaging (MRI), Computerized Tomography (CT) imaging and X Ray imaging for analysis. Both MRI and CT scans are more effective at generating clear images, but they are also quite expensive and expose the patient to radiation. The Chest X Ray (CXR) images are therefore the preferable choice for identification of respiratory diseases or lung disorders. It is possible to classify three lung disorders namely Pneumonia, Tuberculosis and COVID-19 by analyzing CXR images of patients.

Deep learning is highly efficient and produce better results for classification of CXR images [9]. Deep learning has achieved substantial advancements in feature learning and feature representations [19]. It generated possibilities for establishing an automated intelligent model for image related health care solutions [17]. For example, several deep learning-based analysis of medical images [2,31,34] was developed to automatically learn significant features from image for detection of diseases thereby preventing severe illness or disorders. The role of features is important in case of deep learning-based classification model. In this research work, a fused feature extraction technique is developed for deep learning based multi-level classification of diseases namely Tuberculosis, Pneumonia and COVID-19.

Related Work

Classification of Chest X Ray images can be done by extracting hand crafted features manually or deep features which can be automatically extracted using neural networks in the deep learning models. A survey of existing techniques for extracting features from X ray images was presented by Salau et al. [44]. It is observed from the survey that most of the researchers utilized Gray Level Difference Statistics (GLDS) features for classification. One of the main components of images is colour, which is specified using any of the following colour spaces or models like Red Green Blue (RGB) and Hue Saturation Value (HSV) etc. [40]. These features can be used for the purpose of classification. An extensive survey of methods to extract texture features from the images was presented by Humeau et al. [25]. Both the fuzzy set theoretical approach and the histogram pixel method of extraction have been used however they are incredibly unsuited to noisy situations [50]. Features such as Global texture (curvelet) features and colour features can be used for image retrieval [54],[49] and for image classification. Rakshit et al. [41] coupled texture features with colour features to improve faster image retrieval and the same features can also be utilized for classification. A comparative analysis of various approaches for extracting features from images was presented by Ghosh et al. [16]. Feature extraction techniques such as statistical methods [8], [42], [12] can be used to extract some properties which are not identified easily. This contains neighbourhood grey tone difference, First Order Statistics (FOS), Grey Level Co-Occurrence Matrix (GLCM), and Grey Level Run Length Matrix (GLRLM).

A specialized deep network coupled with single transfer learning method was implemented to construct a mobile application namely "MobApp4InfectiousDisease"[32]. As a result of experimentation, MobApp4InfectiousDisease achieves accuracy of 97.72% and the outcomes are also compared with traditional methods. Deep learning based multi classification system for automatic classification of CXR images was created by Malik et al. [38]. The system helps to classify or identify diseases such as Lung Cancer (LC), Pneumothorax, Tuberculosis (TB), Pneumonia and COVID-19. Detection of COVID-19 and related illnesses was done by Chest Disease Classifier Network (CDC Net), a Convolutional Neural Network (CNN) which includes residual network ideas with dilated convolution. In order to classify and identify pulmonary disorders including COVID-19, pneumonia and tuberculosis, deep features from CXR images are extracted using a deep neural network (DNN) model [9]. Deep networks such as ResNet50, ResNet152V2, InceptionV3 and MobileNetV2 are used in the proposed DNN model. A deep transfer learning based Conditional Generative Adversarial Network (cGAN) is utilized to categorize CXR images into six types namely Normal, Pneumonia, Tuberculosis, COVID-Mild, COVID-Medium, and COVID-Severe [37]. A Convolutional Neural Network (CNN) model is utilized by Bhandari et al. [7] to detect Pneumonia, COVID-19 and Tuberculosis by analyzing CXR images. The authors integrate CNN model with eXplainable Artificial Intelligence (XAI) framework and achieves an accuracy of 94.54%.

A hybrid deep network is built by concatenating two models namely VGG16 and VGG19 to detect diseases namely COVID-19, Pneumonia and Tuberculosis. Hybrid models extract deep features from CXR images and achieves an accuracy of 99.66% [15]. To classify COVID-19, a deep learning model with two phases namely "Mask Attention Network (MANet)" was developed by Xu et al. [55]. "MANet" classifies COVID-19 from classes like Normal, Tuberculosis (TB), Bacterial Pneumonia (BP), and Viral Pneumonia (VP). Mask Attention Network is integrated with architectures of Convolutional Neural Network namely ResNet34, ResNet50, VGG16, and Inceptionv3. Out of all classifiers, ResNet50 with MANet provides better accuracy which is 96.32%. To classify diseases such as Pneumonia, Tuberculosis and COVID-19, Kong et al. [29] developed a deep learning model by implementing feature fusion of Dense Convolutional Network (DNN) and VGG16. Sultana et al. [48] introduced a framework to classify diseases such as COVID-19, Tuberculosis, Pneumonia using Deep Convolutional Neural Network (DNN). A deep transfer learning network to classify Pneumonia, COVID-19, Tuberculosis namely "DenResCov-19" is developed by Mamalakis et al. [36]. DenResCov-19 is generated by combining DenseNet -121 and ResNet -50 networks. Using CXR images, DenResCov-19 can determine whether the person is normal or affected by COVID-19, pneumonia, TB.

Materials And Methodology

This section describes about the Dataset description and the steps involved in multi-level lung disease classification. The outline of the research work is shown in Figure 2. Chest X ray images of several lung disorders such as COVID-19, Tuberculosis and Pneumonia are obtained from NIH database. The collected CXR images undergo preprocessing and data augmentation so that the images can be resized and normalized. Then, the features are extracted from CXR images using fused feature extraction technique. Finally, multi-level classification is performed using the fused features and the performance is evaluated using various metrics.

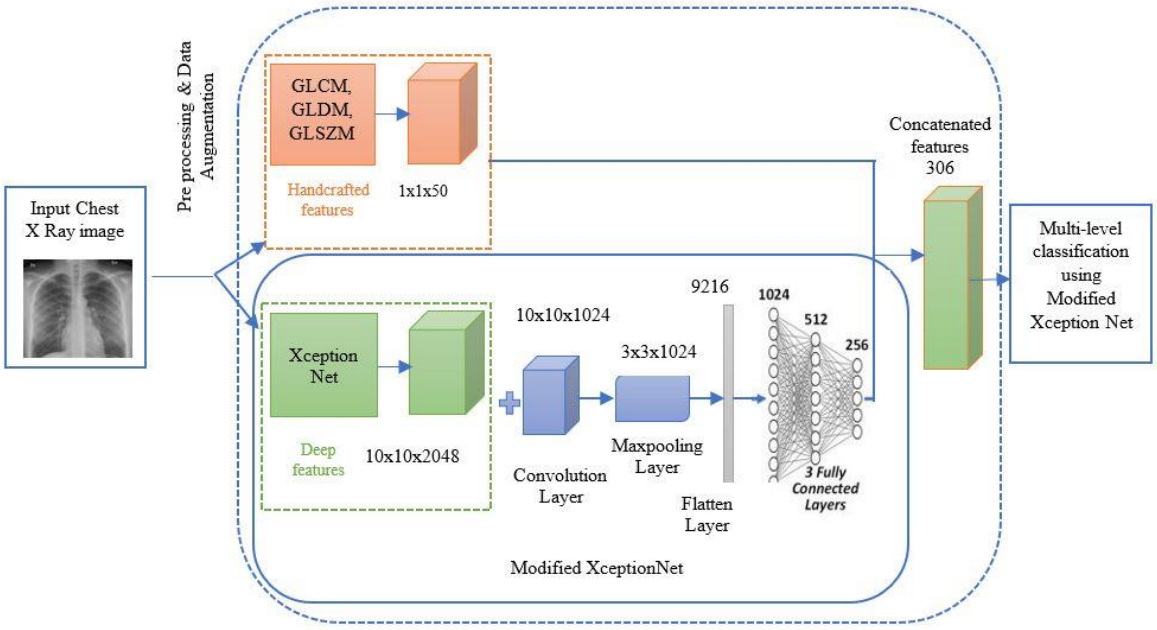

Figure 2. Overview of the work

XceptionNet produces a 10x10x2048 feature map at the last feature extraction layer. In the proposed model, deep features are passed through convolution layer, max pooling layer and dense layers, then the features are concatenated with the handcrafted features and fed into the classifier for multi-level classification.

Dataset Description

The dataset used for training and testing in this research is accessible to everyone on National Institute of Health (NIH) - Kaggle [23]. Few sample input images are collected from Kaggle dataset is shown in Figure 3. The Kaggle dataset is made up of several smaller datasets which includes the categories namely Normal, Tuberculosis, Pneumonia and COVID-19.

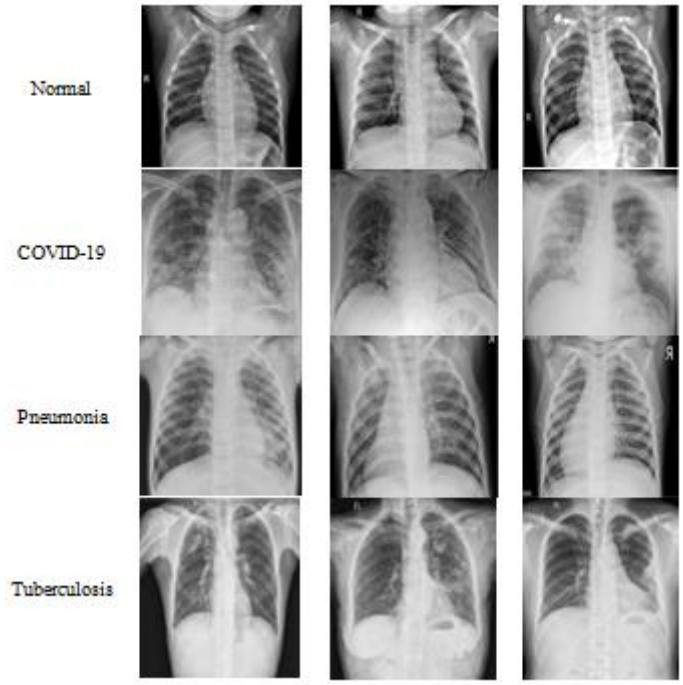

Figure 3. Sample images from the Dataset

Total number of CXR images acquired from the dataset is 16000. The dataset is split into training data and testing data where 70% is for training and 30% is for testing. The details of the dataset with classes and number of images is shown in Table 1.

Table 1. Dataset Description

Dataset	Class		No. of images in the class	No. of images for training set	No. of images for testing set
NIH (Kaggle)	Normal		2228	1560	668
	Tuberculosis		5352	3746	1606
	Pneumonia	Bacterial Pneumonia	2856	1999	857
		COVID-19	5564	3895	1669

3.2 Data pre-processing

Several algorithms require input images with different size and formats and so the images must be normalized according to the standards of deep learning models. Data pre-processing helps to resize the original input CXR images. In pre-processing, the input images with different original sizes are processed and resized uniformly by altering the dimensions of the image to 299 × 299 pixels.

3.3 Data augmentation

Deep learning models usually need lot of training data. Image augmentation is the technique to enhance the diversity and sufficiency of training data by applying random modifications such as image rotation and image flipping etc. Image augmentation helps to develop an efficient deep learning model. The performance of the model is directly proportional to the size of the training data. In this research, three augmentation techniques are utilized: Image rotation with an angle between − 10 and + 10 degrees, horizontal flips and then image noising. After applying data augmentation technique, the model is more efficient and flexible to informational changes.

Proposed Feature Extraction technique - Fusion of Handcrafted and Deep features (FHD)

The proposed FHD technique combines handcrafted features with deep features extracted from CXR images. Handcrafted features are extracted manually from the images whereas deep features are extracted automatically

by the deep network models. Both handcrafted features and deep features has its own advantages and offer better classification outcomes. The combination of both set of features can improve the performance of classification.

Handcrafted Features

Handcrafted features are the features that can be extracted using the direct information present in the images. In this research, feature extraction technique extracts 50 texture features as handcrafted features from CXR images by using methods such as Gray-Level Co-occurrence Matrix (GLCM), Gray Level Difference Matrix (GLDM) and Gray Level Size Zone Matrix (GLSZM).

Gray-Level Co-occurrence Matrix (GLCM)

Gray-Level Co-occurrence Matrix is a technique for analyzing texture of an image. The relationship between adjacent pixels which has varied grey level intensities, angles, and distances is represented by GLCM. GLCM extracts texture features from the image by generating a histogram of co-occurring gray scale values [18]. In general, GLCM extracts features such as correlation, dissimilarity, and homogeneity etc. GLCM helps to extract 20 features from CXR images. The features along with the formula is listed in Table 2.

Table 2. Features extracted using GLCM

Sl.No.	Feature Label	Feature	Formula
1	ENE	Energy	$ENE = \sum_{m=1}^{C_g}\left\{\sum_{n=1}^{C_g}\left\{\left[P_{m,n}\right]^2\right\}\right\}$
2	ENT	Entropy	$ENT = -\sum_{m=1}^{C_g}\left\{\sum_{n=1}^{C_g}\left\{P_{m,n}.\,ln\left[P_{m,n}\right]\right\}\right\}$
3	CONT	Contrast	$CONT = \sum_{m=1}^{C_g}\left\{\sum_{n=1}^{C_g}\left\{(m-n).P_{m,n}\right\}\right\}$
4	CRN	Correlation	$CRN = \frac{\sum_{m=1}^{C_g}\left\{\sum_{n=1}^{C_g}\left\{m.n.P_{m,n}\right\}\right\} - u_i\,.\,u_j}{v_i.v_j}$
5	H	Homogeneity	$H = \sum_{m=1}^{C_g}\frac{P_m}{1+\lvert m\rvert^2}$
6	ASM	Angular Second Moment	$ASM = \sum_{m=1}^{C_g}\left\{\sum_{n=1}^{C_g}\left\{\left(P_{m,n}\right)^2\right\}\right\}$
7	SSV	Sum of Squares variance	$SSV = \sum_{m=1}^{C_g}\left\{\sum_{n=1}^{C_g}\left\{(m-u)^2.P_{m,n}\right\}\right\}$
8	IDM	Inverse Different Moment	$IDM = \sum_{m=1}^{C_g}\left\{\sum_{n=1}^{C_g}\left\{\frac{1}{1+(m-n)^2}.P_{m,n}\right\}\right\}$
9	SAVE	Sum Average	$SAVE = \sum_{k=2}^{2-C_g} k.P_{i+j}\,(k)$
10	SVAR	Sum Variance	$SVAR = \sum_{k=2}^{2-C_g}\left\{(k-SAVE)^2\,.P_{i+j}(k)\right\}$
11	SENT	Sum Entropy	$SENT = \sum_{k=2}^{2-C_g}\left\{P_{i+j}(k).\ln\left[P_{i+j}(k)\right]\right\}$

12	DVAR	Difference Variance	$DVAR = -\sum_{k=0}^{C_{g-1}} \{(k - u_{i-j})^2 . P_{i-j}(k)\}$
13	DENT	Difference Entropy	$DENT = -\sum_{k=0}^{C_{g-1}} \{P_{i-j}(k).\ln[P_{i-j}(k)]\}$
14	IC	Information Correlation	$IC = \frac{Ent - Ent_{ij,1}}{\max\{Ent_i; Ent_j\}}$
15	AC	Auto Correlation	$AC = \sum_{m=1}^{C_g}\left\{\sum_{n=1}^{C_g}\{m.n.P_{m,n}\}\right\}$
16	DS	Dissimilarity	$DS = \sum_{m=1}^{C_g}\left\{\sum_{n=1}^{C_g}\{\lvert m-n\rvert.P_{m,n}\}\right\}$
17	CS	Cluster Shade	$CS = \sum_{m=1}^{C_g}\left\{\sum_{n=1}^{C_g}\{(m+n-u_i-u_j)^3.P_{m,n}\}\right\}$
18	CP	Cluster Prominence	$CP = \sum_{m=1}^{C_g}\left\{\sum_{n=1}^{C_g}\{(m+n-u_i-u_j)^4.P_{m,n}\}\right\}$
19	MP	Maximum Probability	$MP = \max_{m,n}\{P_{m,n}\}$
20	ID	Inverse Difference	$ID = \sum_{m=1}^{C_g}\left\{\sum_{n=1}^{C_g}\left\{\frac{1}{1+(m-n)}.P_{m,n}\right\}\right\}$

GLCM matrix is represented as Pm,n where m and n are the gray level values of the image respectively. Cg refers to the number of discrete gray levels in the image. For the feature correlation, the following formulas can be used.

$$P_{i+j}(k) = \sum_{m=1}^{C_g}\sum_{n=1}^{C_g} P_{mn} \quad \text{where m+n=k, k=2,3,…….}2C_g \tag{1}$$

$$P_{i-j}(k) = \sum_{m=1}^{C_g}\sum_{n=1}^{C_g} P_{mn} \quad \text{where m-n=k, k=0,1,…….}C_g\text{-1} \tag{2}$$

$$u_i = \sum_{m=1}^{C_g}\left\{m.\sum_{n=1}^{C_g}\{P_{m,n}\}\right\} \tag{3}$$

$$u_j = \sum_{n=1}^{C_g}\left\{n.\sum_{n=1}^{C_g}\{P_{m,n}\}\right\} \tag{4}$$

$$v_i = \left(\sum_{m=1}^{C_g}\left\{(m-u_i)^2.\sum_{n=1}^{C_g}\{P_{m,n}\}\right\}\right)^{1/2} \tag{5}$$

$$v_j = \left(\sum_{n=1}^{C_g}\left\{(n-u_j)^2.\sum_{m=1}^{C_g}\{P_{m,n}\}\right\}\right)^{1/2} \tag{6}$$

(6)

Gray Level Dependence Matrix

Gray Level Dependence Matrix (GLDM) [51] measures the dependencies within the gray levels of an image. The matrix is used to determine the number of voxels (pixel + volume) depend on the central voxel of the image. Let P (m,n) be the Gray level dependence matrix, (m,n)th element describes the frequency of voxels with gray level m dependent voxels n in its neighbourhood present in the image.

Let D be the input image. Let D_g be the number of discrete intensity values in D, D_d quantifies the discrete dependency sizes in D and D_z refers to the amount of dependency zones in D. The texture features extracted using GLDM are listed in Table 3.

Table 3. Features extracted using GLDM

Sl.No.	Feature Label	Feature	Formula
1	SDE	Small Dependence Emphasis	$SDE = \frac{\sum_{m=1}^{D_g}\sum_{n=1}^{D_d}\frac{P_{m,n}}{m^2}}{D_z}$
2	LDE	Large Dependence Emphasis	$LDE = \frac{\sum_{m=1}^{D_g}\sum_{n=1}^{D_d}P(m,n)n^2}{D_z}$
3	GLN	Gray Level Non-Uniformity	$GLN = \frac{\sum_{m=1}^{D_g}\left(\sum_{n=1}^{D_d}P(m,n)\right)^2}{D_z}$
4	DN	Dependence Non-Uniformity	$DN = \frac{\sum_{n=1}^{D_d}\left(\sum_{m=1}^{D_g}P(m,n)\right)^2}{D_z}$
5	DNN	Dependence Non-Uniformity Normalized	$DNN = \frac{\sum_{n=1}^{D_d}\left(\sum_{m=1}^{D_g}P(m,n)\right)^2}{{D_z}^2}$
6	GLV	Gray Level Variance	$GLV = \sum_{m=1}^{D_g}\sum_{n=1}^{D_d}P(m,n)\,(m - \left(\sum_{m=1}^{D_g}\sum_{n=1}^{D_d}mP(m,n)\right)$
7	DV	Dependence Variance	$DV = \sum_{m=1}^{D_g}\sum_{n=1}^{D_d}P(m,n)\,(n - \left(\sum_{m=1}^{D_g}\sum_{n=1}^{D_d}nP(m,n)\right)$
8	DE	Dependence Entropy	$DV = -\sum_{m=1}^{D_g}\sum_{n=1}^{D_d}P(m,n)\,(log_2\,(p(m,n)+\in)$
9	LGLE	Low Gray Level Emphasis	$LGLE = \frac{\sum_{m=1}^{D_g}\sum_{n=1}^{D_d}\frac{P(m,n)}{m^2}}{D_z}$
10	HGLE	High Gray Level Emphasis	$HGLE = \frac{\sum_{m=1}^{D_g}\sum_{n=1}^{D_d}P(m,n)m^2}{D_z}$
11	SDLGLE	Small Dependence Low Gray Level Emphasis	$SDLGLE = \frac{\sum_{m=1}^{D_g}\sum_{n=1}^{D_d}\frac{P(m,n)}{m^2n^2}}{D_z}$
12	SDHGLE	Small Dependence High Gray Level Emphasis	$SDHGLE = \frac{\sum_{m=1}^{D_g}\sum_{n=1}^{D_d}\frac{P(m,n)m^2}{n^2}}{D_z}$
13	LDLGLE	Large Dependence Low Gray Level Emphasis	$LDLGLE = \frac{\sum_{m=1}^{D_g}\sum_{n=1}^{D_d}\frac{P(m,n)n^2}{m^2}}{D_z}$

14	LDHGLE	Large Dependence High Gray Level Emphasis	$LDHGLE = \frac{\sum_{m=1}^{D_g}\sum_{n=1}^{D_d} P(m,n)m^2n^2}{D_z}$

Where ∈ is the arbitrarily small positive number (~2.2 X 10-16), P(m,n) represents the dependence matrix and p(m,n) indicates the normalized dependence matrix.

$$p(m,n) = \frac{P(m,n)}{D_z} \quad (7)$$

Number of dependency zones (D_Z) in the D is calculated using following equation

$$D_Z = \sum_{m=1}^{D_g}\sum_{n=1}^{D_d} P(m,n) \quad (8)$$

Gray Level Size Zone Matrix

Gray Level Size Zone Matrix (GLSZM) [3] represents or measures the gray level zone in an image. The quantity of connected voxels with the same gray level intensity makes up a gray level zone. Let us consider P(m,n) refers to gray level size zone matrix where (m,n)th element refers to the amount of zones which has gray level m and size n in the image.

Let S be the input image. Let S_g be the number of discrete intensity values in S, S_s be the number of discrete zone sizes in S and S_z refers to the number of zones in S. The list of features extracted using GLSZM is shown in Table 4.

Table 4. Features extracted using GLSZM

Sl.No.	Feature Label	Feature	Formula
1	SAE	Small Area Emphasis	$SDE = \frac{\sum_{m=1}^{S_g}\sum_{n=1}^{S_s}\frac{P_{m,n}}{m^2}}{S_z}$
2	LAE	Large Area Emphasis	$LDE = \frac{\sum_{m=1}^{S_g}\sum_{n=1}^{S_s} P(m,n)n^2}{S_z}$
3	GLN	Gray Level Non-Uniformity	$GLN = \frac{\sum_{m=1}^{S_g}\left(\sum_{n=1}^{S_s} P(m,n)\right)^2}{S_z}$
4	GLNN	Gray Level Non-Uniformity Normalized	$GLNN = \frac{\sum_{m=1}^{S_g}\left(\sum_{n=1}^{S_s} P(m,n)\right)^2}{{S_z}^2}$
5	SZN	Size Zone Non-Uniformity	$SZN = \frac{\sum_{n=1}^{S_s}\left(\sum_{m=1}^{S_g} P(m,n)\right)^2}{S_z}$

6	SZNN	Size Zone Non-Uniformity Normalized	$SZNN = \frac{\sum_{n=1}^{S_s}\left(\sum_{m=1}^{S_g} P(m,n)\right)^2}{{S_z}^2}$
7	ZP	Zone Percentage	$ZP = \frac{N_z}{N_p}$
8	GLV	Gray Level Variance	$GLV = \sum_{m=1}^{S_g}\sum_{n=1}^{S_s} p(m,n)(m - \left(\sum_{m=1}^{S_g}\sum_{n=1}^{S_s} p(m,n)m\right))^2$
9	ZV	Zone Variance	$ZV = \sum_{m=1}^{S_g}\sum_{n=1}^{S_s} p(m,n)(m - \left(\sum_{m=1}^{S_g}\sum_{n=1}^{S_s} p(m,n)n\right))^2$
10	ZE	Zone Entropy	$ZE = \sum_{m=1}^{S_g}\sum_{n=1}^{S_s} P(m,n)\ (log_2\ (p(m,n)+\in)$
11	LGLZE	Low Gray Level Zone Emphasis	$LGLZE = \frac{\sum_{m=1}^{S_g}\sum_{n=1}^{S_s}\frac{P(m,n)}{m^2}}{S_z}$
12	HGLZE	High Gray Level Zone Emphasis	$HGLE = \frac{\sum_{m=1}^{S_g}\sum_{n=1}^{S_s} P(m,n)m^2}{S_z}$
13	SALGLE	Small Area Low Gray Level Emphasis	$SALGLE = \frac{\sum_{m=1}^{S_g}\sum_{n=1}^{S_s}\frac{P(m,n)}{m^2n^2}}{S_z}$
14	SAHGLE	Small Area High Gray Level Emphasis	$SAHGLE = \frac{\sum_{m=1}^{S_g}\sum_{n=1}^{S_s}\frac{P(m,n)m^2}{n^2}}{S_z}$
15	LALGLE	Large Area Low Gray Level Emphasis	$LALGLE = \frac{\sum_{m=1}^{S_g}\sum_{n=1}^{S_s}\frac{P(m,n)n^2}{m^2}}{S_z}$
16	LAHGLE	Large Area High Gray Level Emphasis	$LAHGLE = \frac{\sum_{m=1}^{S_g}\sum_{n=1}^{S_s} P(m,n)m^2n^2}{S_z}$

Where $\in$ is the arbitrarily small positive number (~2.2 X 10^{-16}), P(m,n) refers to the size zone matrix and p(m,n) is the normalized size zone matrix.

$$p(m,n) = \frac{P(m,n)}{S_z} \quad (9)$$

The number of zones (S_Z) in the image is computed using the following equation

$$S_Z = \sum_{m=1}^{S_g} \sum_{n=1}^{S_s} P(m,n) \tag{10}$$

The number of zones (S_Z) in the image is computed using the following equation

Deep features

Deep features are extracted using Modified XceptionNet [14], a Convolutional Neural Network (CNN) model. XceptionNet architecture with depth-wise separable convolutions was introduced by Chollet [9]. It is also identified that XceptionNet provides better results on ImageNet dataset [11][30]. Each deep learning model consists of feature extraction layer which are placed in front of the dense layers. The feature extraction layer is utilized to extract features whereas the dense layers are intended for classification. In order to extract features, XceptionNet architecture consists of 36 convolutional layers. The 36 convolution layers of XceptionNet is organized into 14 different modules which are connected to one another by linear skips except the first and last module. The features from the input CXR are extracted using the convolution layers. The depth wise separable convolutions together with the residual connection makes the XceptionNet to learn and extract features efficiently [46]. In XceptionNet, depth wise separable convolutions initially perform spatial convolutions on each channel of input layer and then apply point wise convolution in order to merge the various outputs of channel into single one. The 36 convolutional layers of XceptionNet is divided into three modules which are as follows.

Entry flow contains 8 convolution layers
Middle flow includes 24 convolution layers which are contained in eight blocks with three layers each.
Exit flow contains 4 convolution layers.
Modified XceptionNet consists of an additional convolutional layer and Max pooling layer. The input image sequentially moves through all the three modules. In this research work, 256 deep features are extracted using Modified XceptionNet.

Fusion of Handcrafted and Deep features

The set of features extracted from CXR images are called as Feature Vector. The performance of the classifier strongly depends on the input Feature Vector. The handcrafted Feature Vector and the Deep Feature Vector are fused together and fed into Modified XceptionNet classifier to obtain the classified output. This concatenation of Feature Vectors provides better classification results than individual Feature Vector as integration of two different Feature Vectors take the advantages of different feature extraction methods. Independent Feature Vector acquired using proposed FHD feature extraction technique is defined in Equation 9 which represents 50 gray level-based texture features extracted from input CXR images. Feature Vector obtained using Modified XceptionNet model is defined in Equation 10 which represents 256 deep features extracted from the input CXR images. A new Feature Vector is generated by the concatenation of individual Feature Vectors and is defined in Equation 11.

$$FV_{FGLT(N\times 50)} = (FGLT_{N\times 1}, FGLT_{N\times 2}, FGLT_{N\times 3} \dots \dots \dots . FGLT_{N\times 50}) \tag{9}$$

$$FV_{MX(N\times 256)} = (MX_{N\times 1}, MX_{N\times 2}, MX_{N\times 3} \dots \dots \dots . MX_{N\times 256}) \tag{10}$$

$$EFV_{N\times 306} = \sum_{i=1}^{N} (FV_{FGLT}, FV_{MX}) \tag{11}$$

Where MX refers to Modified XceptionNet, N represents number of classes. For triclass classification, the value of N is 3 and the value is 2 for binary classification and EFV represents the Ensemble Feature Vector

Multi-level classification using Deep learning

Multi-level classification consists of two phases which are named as first level and second level of classification. The first level is for classification of input CXR images into 3 classes namely Normal, Tuberculosis and Pneumonia. Taking the pneumonia classified CXR images as input, the second level of classification is used to classify the types of pneumonia into 2 classes namely Bacterial pneumonia and COVID-19. The flow of multi-level classification is shown in Figure 4.

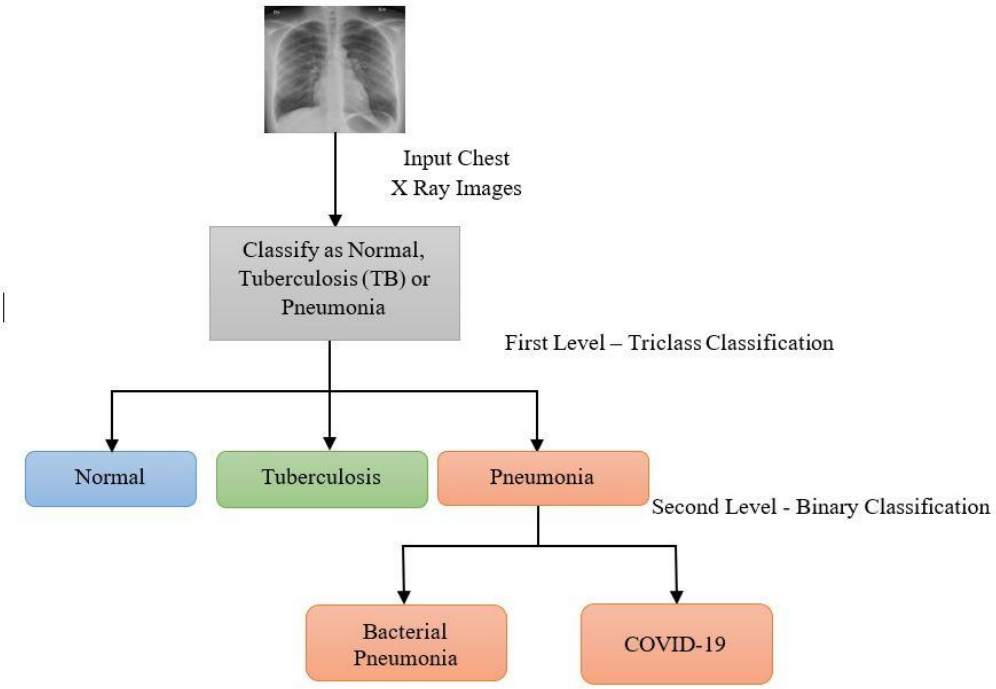

Figure 4. Multi-level classification

After the fusion of handcrafted and deep features, a Modified XceptionNet was built and the network is trained for Triclass classification with three classes (Normal, Tuberculosis and Pneumonia). After the training of model, it was tested using the testing set. Images which are identified as pneumonia in the first level classification are saved and the same is used as testing set in second level binary classification to classify the pneumonia images into bacterial pneumonia or COVID-19. The pseudocode of the proposed method is provided below.

Pseudocode of the proposed method

*Step 1: Input: Chest X Ray images from NIH-Kaggle dataset of size 1024*1024*

*Step 2: Pre-processing: Resize the input images to 299*299*3*

Step 3: Perform Data Augmentation using RandAugment function for Image Rotation, Horizontal Flip and Image Noising.

Step 4: Split train data to (70,30): 70% for training and 30% for testing.

Step 5: Extract handcrafted texture features using GLCM,GLDM and GLSZM.

Step 6: Extract deep features using Modified XceptionNet.

Step 7: Perform fusion of handcrafted and deep features by generating Ensemble Feature Vector (EFV) using Equation 11.

Step 8: Input the fused features to the Modified XceptionNet for triclass classification (Normal, Tuberculosis, Pneumonia).

Step 9: Implement Binary classification (Bacterial Pneumonia, COVID-19) using Modified XceptionNet if the output of triclass classification is Pneumonia.

Step 10: Evaluate the performance of multilevel classification using performance metrics

The parameters utilized in the proposed method are shown in Table 5.

Table 5. Parameters for classification using Modified XceptionNet

Parameters	Value
Image Shape	299X299X3
Data Augmentation	RandAugment
Base Model	Modified XceptionNet
Classifier	Softmax
Optimizer	Nadam
Loss function	Categorical Crossentropy
Class	Triclass and Binary class
Learning rate	0.01
Dropout	0.5
Epoch	25 to 100
Batch Size	32

Based on Table 5, Categorical Cross entropy loss function and Nadam optimizer is utilized to train the modified XceptionNet. Nadam is used to optimize the training process of modified XceptionNet which helps to improve the accuracy and running time of the neural network. In each training phase, the neural network is trained with 100 epochs. The learning rate and the batch size was set to 0.01 and 32 respectively.

Experimental Results and Performance Evaluation of proposed FHD

The input CXR images are acquired from NIH - Kaggle dataset [23] and the details about the number of samples in each class is provided in Table 1.

Performance Metrics

The performance of the proposed FHD feature extraction technique is evaluated with Modified XceptionNet using performance metrics such as Accuracy, Precision, Recall, Specificity, F-measure and Error rate. The formula to compute performance metrics is shown in Table 6.

Table 6. Performance Metrics

Metrics	Description	Formula
Accuracy	Ratio of number of correct predictions or observations to all observations	$Accuracy = \frac{TP + TN}{TP + FP + TN + FN}$
Precision	Proportion of number of true positive predictions to the sum of expected true positive observations	$Precision = \frac{TP}{TP + FP}$
Recall	Ratio of number of correctly predicted true positives to all correct observations	$Recall = \frac{TP}{TP + FN}$
Specificity	Ratio of amount of true negative predictions to the number of wrong observations	$Specificity = \frac{TN}{TN + FP}$
F-measure	Weighted average of Precision and Recall and this score accounts for both false positives and false negatives	$F - measure = 2 * \frac{Precision * Recall}{Precision + Recall}$
Error Rate	Refers to the number of observations that are misclassified.	$Error\ Rate = 1 - \frac{TP + TN}{TP + FP + TN + FN}$

Where TP, TN, FP and FN refer to True Positive, True Negative, False Positive and False Negative respectively. The confusion matrix [6] is a matrix with TP,TN,FP and FN as its elements and helps to calculate the performance metrics to evaluate the classification model. The confusion matrix of first level classification using Modified XceptionNet and proposed FHD with classes Normal, Tuberculosis and Pneumonia is shown in Figure 5 and the confusion matrix for second level classification using Modified XceptionNet and proposed FHD with classes Bacterial pneumonia and COVID-19 is given in Figure 6.

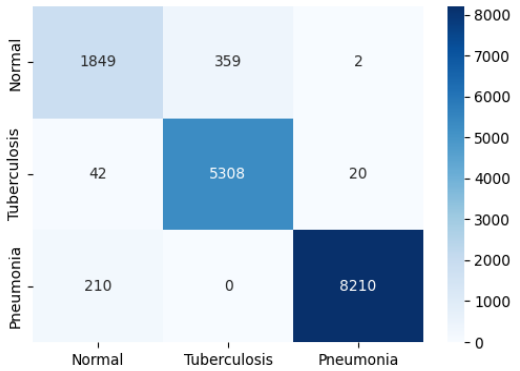

Figure 5. Confusion matrix for Triclass using Modified XceptionNet and proposed FHD

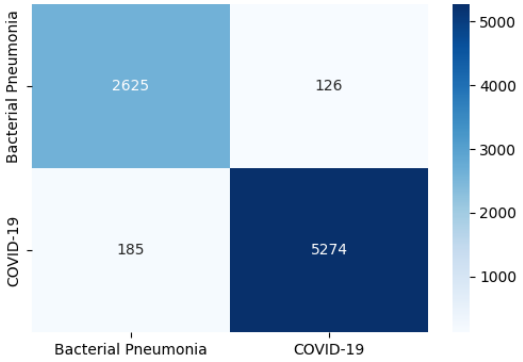

Figure 6. Confusion matrix for Binary class using Modified XceptionNet and proposed FHD

Figure 5 represents the confusion matrix of first level classification which contains 3 classes. From the figure, it is observed that the Modified XceptionNet model with the proposed FHD correctly predicts 1849 images as Normal class out of 2210 images whereas 359 normal images are assumed as tuberculosis and 2 normal images are assumed as pneumonia. The model correctly identifies 5308 images as Tuberculosis class out of 5370 while 42 images are wrongly identified as Normal and 20 images are wrongly identified as pneumonia. 8210 images out of 8420 images are correctly predicted as pneumonia class whereas the remaining 210 images are assumed as normal class. Second level classification is the binary classification with classes Bacterial pneumonia and COVID-19. Confusion matrix for second level of classification is presented in Figure 6. In Bacterial pneumonia class, 2625 images are correctly predicted as Bacterial pneumonia and 126 images are wrongly predicted as COVID-19. Similarly, in COVID-19 class, 5274 images are classified correctly as COVID-19 whereas 185 images are wrongly predicted as Bacterial pneumonia. The performance metrics are calculated and the results are presented in Table 6 and Table 7.

Experimental results of the proposed FHD with Modified XceptionNet classifier is presented in Table 6. It is observed that the concatenation of handcrafted and deep features outperforms individual set of features for both first level and second level classification. Fused features provide an accuracy of 96% for triclass classification which is the first level classification and 96.2% for binary classification which belongs to second level classification.

Table 6. Experimental results of proposed FHD with Modified XceptionNet classifier

Classification	Feature set	Method	Accuracy	Precision	Recall	Specificity	F-measure	Error Rate
First Level classification	Handcrafted Features	GLCM	92.40	89.92	90.14	92.96	90.46	7.60
		GLDM	90.88	88.26	89.10	90.98	88.80	9.12

	(HF)	GLSZM	89.67	86.42	87.56	89.92	87.72	10.33
	Deep Features (DF)	Modified XceptionNet	94.20	91.18	92.26	94.92	92.34	5.80
	Fused Features	HF+DF	**96.04**	93.65	94.59	96.78	94.12	3.96
Second Level classification	Handcrafted Features (HF)	GLCM	94.26	92.88	93.10	94.98	94.38	5.74
		GLDM	92.62	90.44	91.42	92.88	92.46	7.38
		GLSZM	90.82	88.16	89.67	90.99	90.68	9.18
	Deep Features (DF)	Modified XceptionNet	95.40	93.29	92.34	95.82	95.66	4.60
	Fused Features	HF+DF	**96.20**	94.08	94.61	96.99	94.34	3.80

Table 7. Experimental results of proposed FHD with various classifiers

Classification	Deep learning model	Accuracy	Precision	Recall	Specificity	F-measure	Error Rate
First level classification	VGG16	92.28	90.00	90.64	92.94	90.22	7.72
	ResNet50	88.68	86.29	90.12	88.96	86.82	11.32
	MobileNetV2	94.28	92.14	93.46	94.88	93.10	5.72
	Modified XceptionNet	**96.04**	93.65	94.59	96.78	94.12	3.96
Second level classification	VGG16	94.62	92.68	93.19	94.98	92.94	5.38
	ResNet50	90.92	88.88	89.23	90.99	89.10	9.08
	MobileNetV2	96.00	94.68	94.92	96.16	94.88	4.00
	Modified XceptionNet	**96.20**	94.08	94.61	96.99	94.34	3.80

It is inferred from Table 7 that, Modified XceptionNet provides better classification than other deep learning models for both level of classification. Modified XceptionNet outperforms other models and provides an average accuracy of 96.2%. Comparison of average accuracy of all the four deep learning models for handcrafted features, deep features and the proposed fused features is presented in Figure 7.

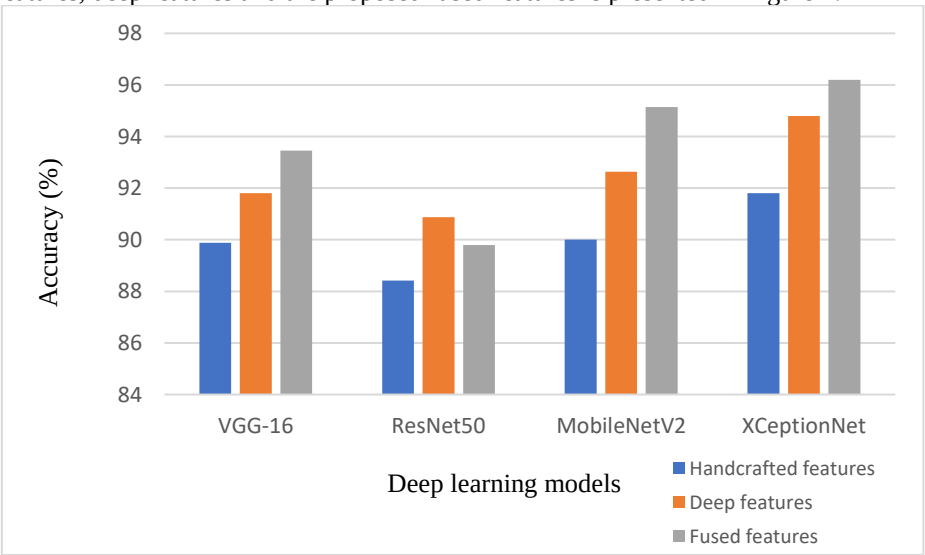

Figure 7. Average accuracy of deep learning models for handcrafted, deep and fused features

The proposed fused features provide better classification accuracy in all deep learning models except ResNet50. It is also observed that Modified XceptionNet proved to be the best classifier as it provides highest accuracy for handcrafted, deep and fused features. The performance of proposed FHD is evaluated using Modified XceptionNet classifier for different number of epochs and the outcome is shown in Figure 8. Training phase includes 70% of the dataset and 30% is for testing.

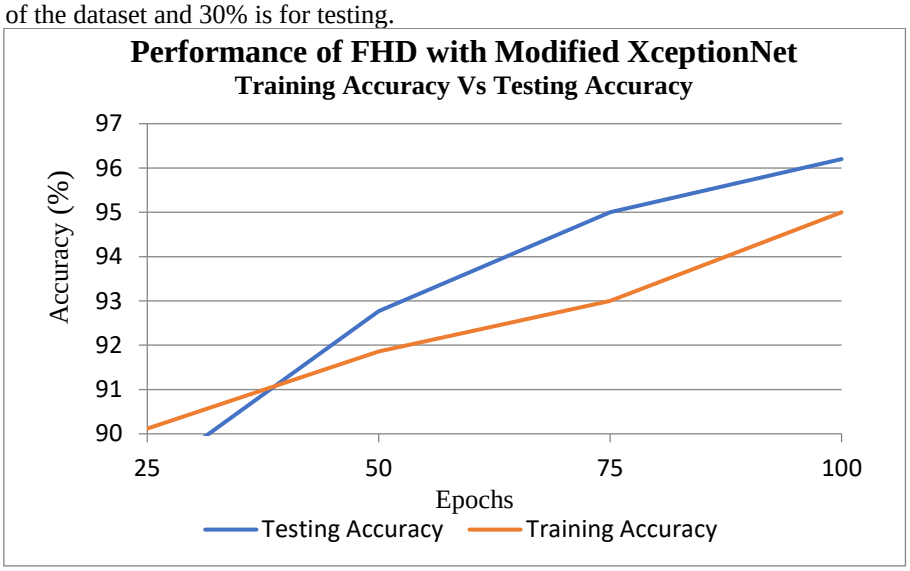

Figure 8. Performance of proposed FHD with Modified XceptionNet for various epochs

It is observed from Figure 8 that, performance of the classifier increases with number of epochs. As a result of experimentation for various epochs, Modified Xception Net provides an accuracy of 95% in training and accuracy of 96.2% in testing for 100 epochs. The performance of proposed FHD with Modified XceptionNet is compared with few existing models and the results are provided in Table 8.

Table 8. Comparison of proposed FHD with Modified XceptionNet and existing models

Sl.No.	Reference	Method for feature extraction	Classification model	Accuracy (%)
1	Shankar, K., and Eswaran Perumal [47]	Handcrafted features (LBP) + Deep features (Inception V3)	Neural Network (MultiLayer Perceptron (MLP))	94.08
2	Ayaz et al. [5]	Handcrafted features (Gabor filter) + Deep features (Inception V3)	Inception V3	86.23
3	Ho et al. [20]	Handcrafted features (Local descriptors, Radiomics features) + Deep features (ResNet18+DenseNet121)	ResNet18+DenseNet121	94.10
4	Li et al. [26]	Handcrafted features (SIFT&Gabor) + Deep features (RibCage Network (RC Net))	RibCage Network (RC Net)	94.10
5	Zhang et al. [57]	Handcrafted features (Local Binary Pattern (LBP) & Bag of Features (BoF)) + Deep features	Deep Convolutional Neural Network (DCNN)	85.47
6	Nanni L.S. et al. [39]	Handcrafted features (Completed Local Binary Pattern (CLBP)) + Deep features (	Convolutional Neural Network (CNN)	96.00

7	Thanga Selvi, R et al. [52]	Handcrafted features (Histogram of Gradients (HoG)) + Deep features (VGG19)	Neural Network (MultiLayer Perceptron (MLP))	94.70
8	Daoud et al. [10]	Handcrafted features (Morphological features) + Deep features (VGG16)	Visual Geometry Group (VGG16)	96.10
9	Liu et al. [32]	Handcrafted features (Local Binary Pattern & Bag of visual words) + Deep features (CNN)	Convolutional Neural Network (CNN)	95.02
10	Proposed FHD	Handcrafted features (GLCM+GLDM+GLSZM) + Deep features (Modified XceptionNet)	Modified XceptionNet	96.20

From Table 8, it is identified that the proposed FHD provides highest accuracy of 96.2% as it combines handcrafted and deep features. The main benefit of proposed FHD is that it extracts 50 handcrafted features using GLCM, GLDM, GLSZM and 256 deep features using Modified XceptionNet model. The second highest accuracy is provided by VGG16 model which is 96.1%.

Conclusion

An efficient feature extraction technique for deep learning based multi-level classification is developed in this research which extracts both handcrafted and deep features from the CXR images and utilize Modified XceptionNet for classification. This research work mainly focuses on fusion of handcrafted and deep features for multilevel classification which contains two levels namely first level classification with three classes such as Normal, Tuberculosis, Pneumonia and second level classification with two classes namely COVID-19 and Bacterial pneumonia. The proposed FHD extracts both handcrafted and deep features from CXR images. The performance of the proposed FHD with Modified XceptionNet is evaluated using performance metrics and it is also compared with other deep learning classification models such as VGG16, ResNet50 and MobileNetV2. With respect to the performance metrics, it is identified that the performance of fused features surpassed the performance of handcrafted and deep features. As a result of experimentation, proposed FHD and Modified XceptionNet outperforms other deep learning models with an accuracy of 96.2%. In future, the number of features can be reduced which will minimize the computational and time complexity and may also improve the classification accuracy.

References

1. Agusti, Alvar, Bartolome R. Celli, Gerard J. Criner, David Halpin, Antonio Anzueto, Peter Barnes, Jean Bourbeau et al. "Global initiative for chronic obstructive lung disease 2023 report: GOLD executive summary." American Journal of Respiratory and Critical Care Medicine 207, no. 7 (2023): 819-837.
2. Ahsan, Md Manjurul, Kishor Datta Gupta, Mohammad Maminur Islam, Sajib Sen, Md Lutfar Rahman, and Mohammad Shakhawat Hossain. "Covid-19 symptoms detection based on nasnetmobile with explainable ai using various imaging modalities." Machine Learning and Knowledge Extraction 2, no. 4 (2020): 490-504.
3. Al-Areqi, Farid, and Mehmet Zeki Konyar. "Effectiveness evaluation of different feature extraction methods for classification of covid-19 from computed tomography images: A high accuracy classification study." Biomedical Signal Processing and Control 76 (2022): 103662.
4. Asif, Hafiz Muhammad, and Hafiz Abdul Sattar Hashmi. "Early detection of COVID-19." (2020).
5. Ayaz, Muhammad, Furqan Shaukat, and Gulistan Raja. "Ensemble learning based automatic detection of tuberculosis in chest X-ray images using hybrid feature descriptors." Physical and Engineering Sciences in Medicine 44, no. 1 (2021): 183-194.
6. Beauxis-Aussalet, Emma, and Lynda Hardman. "Simplifying the visualization of confusion matrix." In 26th Benelux Conference on Artificial Intelligence (BNAIC). 2014.
7. Bhandari, Mohan, Tej Bahadur Shahi, Birat Siku, and Arjun Neupane. "Explanatory classification of CXR images into COVID-19, Pneumonia and Tuberculosis using deep learning and XAI." Computers in Biology and Medicine 150 (2022): 106156.
8. Bhusri, Sahil, Shruti Jain, and Jitendra Virmani. "Classification of breast lesions using the difference of statistical features." (2016).

9. Chollet, François. "Xception: Deep learning with depthwise separable convolutions." In Proceedings of the IEEE conference on computer vision and pattern recognition, pp. 1251-1258. 2017.
10. Daoud, Mohammad I., Samir Abdel-Rahman, Tariq M. Bdair, Mahasen S. Al-Najar, Feras H. Al-Hawari, and Rami Alazrai. "Breast tumor classification in ultrasound images using combined deep and handcrafted features." Sensors 20, no. 23 (2020): 6838.
11. Deng, Jia, Wei Dong, Richard Socher, Li-Jia Li, Kai Li, and Li Fei-Fei. "Imagenet: A large-scale hierarchical image database." In 2009 IEEE conference on computer vision and pattern recognition, pp. 248-255. Ieee, 2009
12. Dhiman, Akanksha, Ambesh Singh, Shwetanjali Dubey, and Shruti Jain. "Design of lead II ECG waveform and classification performance for morphological features using different classifiers on lead II." (2016).
13. Dong, Ke, Chengjie Zhou, Yihan Ruan, and Yuzhi Li. "MobileNetV2 model for image classification." In 2020 2nd International Conference on Information Technology and Computer Application (ITCA), pp. 476-480. IEEE, 2020.
14. El Gannour, Oussama, Soufiane Hamida, Bouchaib Cherradi, Mohammed Al-Sarem, Abdelhadi Raihani, Faisal Saeed, and Mohammed Hadwan. "Concatenation of pre-trained convolutional neural networks for enhanced covid-19 screening using transfer learning technique." Electronics 11, no. 1 (2021): 103
15. El Gannour, Oussama, Soufiane Hamida, Shawki Saleh, Yasser Lamalem, Bouchaib Cherradi, and Abdelhadi Raihani. "COVID-19 detection on X-ray images using a combining mechanism of pre-trained CNNs." International Journal of Advanced Computer Science and Applications 13, no. 6 (2022).
16. Ghosh, Neha, Shikha Agrawal, and Mahesh Motwani. "A survey of feature extraction for content-based image retrieval system." In Proceedings of International Conference on Recent Advancement on Computer and Communication: ICRAC 2017, pp. 305-313. Springer Singapore, 2018.
17. Gu, Jiuxiang, Zhenhua Wang, Jason Kuen, Lianyang Ma, Amir Shahroudy, Bing Shuai, Ting Liu et al. "Recent advances in convolutional neural networks." Pattern recognition 77 (2018): 354-377.
18. Haralick, Robert M., Karthikeyan Shanmugam, and Its' Hak Dinstein. "Textural features for image classification." IEEE Transactions on systems, man, and cybernetics 6 (1973): 610-621.
19. Hinton, Geoffrey E., and Ruslan R. Salakhutdinov. "Reducing the dimensionality of data with neural networks." science 313, no. 5786 (2006): 504-507.
20. Ho, Thi Kieu Khanh, and Jeonghwan Gwak. "Feature-level ensemble approach for COVID-19 detection using chest X-ray images." Plos one 17, no. 7 (2022): e0268430.
21. https://covid19.who.int/
22. https://stoppneumonia.org/latest/world-pneumonia-day-2020
23. https://www.kaggle.com/datasets/nih-chest-xrays/data
24. https://www.who.int/teams/global-tuberculosis-programme/tb-reports/global-tuberculosis-report-2021/disease-burden/mortality
25. Humeau-Heurtier, Anne. "Texture feature extraction methods: A survey." Ieee Access 7 (2019): 8975-9000.
26. Islam, Sheikh Rafiul, Santi P. Maity, Ajoy Kumar Ray, and Mrinal Mandal. "Deep learning on compressed sensing measurements in pneumonia detection." International Journal of Imaging Systems and Technology 32, no. 1 (2022): 41-54.
27. Kallander, Karin, Deborah H. Burgess, and Shamim A. Qazi. "Early identification and treatment of pneumonia: a call to action." The Lancet. Global Health 4, no. 1 (2016): e12.
28. Kaur, Taranjit, and Tapan Kumar Gandhi. "Automated brain image classification based on VGG-16 and transfer learning." In 2019 International Conference on Information Technology (ICIT), pp. 94-98. IEEE, 2019.
29. Kong, Lingzhi, and Jinyong Cheng. "Classification and detection of COVID-19 X-Ray images based on DenseNet and VGG16 feature fusion." Biomedical Signal Processing and Control 77 (2022): 103772.
30. Li, Xuechen, Linlin Shen, Meixiao Shen, and Connor S. Qiu. "Integrating handcrafted and deep features for optical coherence tomography based retinal disease classification." IEEE Access 7 (2019): 33771-33777.
31. Liu, Chang, Yu Cao, Marlon Alcantara, Benyuan Liu, Maria Brunette, Jesus Peinado, and Walter Curioso. "TX-CNN: Detecting tuberculosis in chest X-ray images using convolutional neural network." In 2017 IEEE international conference on image processing (ICIP), pp. 2314-2318. IEEE, 2017.

32. Liu, Dong, Yaohui Liu, Shanglin Li, Weiqing Li, and Luda Wang. "Fusion of handcrafted and deep features for medical image classification." In Journal of Physics: Conference Series, vol. 1345, no. 2, p. 022052. IOP Publishing, 2019.
33. Mahbub, Md Kawsher, Md Zakir Hossain Zamil, Md Abdul Mozid Miah, Partho Ghose, Milon Biswas, and K. C. Santosh. "Mobapp4infectiousdisease: Classify covid-19, pneumonia, and tuberculosis." In 2022 ieee 35th international symposium on computer-based medical systems (cbms), pp. 119-124. IEEE, 2022.
34. Mahbub, Md Kawsher, Milon Biswas, Loveleen Gaur, Fayadh Alenezi, and K. C. Santosh. "Deep features to detect pulmonary abnormalities in chest X-rays due to infectious diseaseX: Covid-19, pneumonia, and tuberculosis." Information Sciences 592 (2022): 389-401.
35. Malik, Hassaan, Tayyaba Anees, Muizzud Din, and Ahmad Naeem. "CDC_Net: Multi-classification convolutional neural network model for detection of COVID-19, pneumothorax, pneumonia, lung Cancer, and tuberculosis using chest X-rays." Multimedia Tools and Applications 82, no. 9 (2023): 13855-13880.
36. Mamalakis, Michail, Andrew J. Swift, Bart Vorselaars, Surajit Ray, Simonne Weeks, Weiping Ding, Richard H. Clayton, Louise S. Mackenzie, and Abhirup Banerjee. "DenResCov-19: A deep transfer learning network for robust automatic classification of COVID-19, pneumonia, and tuberculosis from X-rays." Computerized Medical Imaging and Graphics 94 (2021): 102008.
37. Mehta, Tirth, and Ninad Mehendale. "Classification of X-ray images into COVID-19, pneumonia, and TB using cGAN and fine-tuned deep transfer learning models." Research on Biomedical Engineering 37 (2021): 803-813.
38. Murtaza, Ghulam, Liyana Shuib, Ainuddin Wahid Abdul Wahab, Ghulam Mujtaba, Ghulam Mujtaba, Henry Friday Nweke, Mohammed Ali Al-garadi, Fariha Zulfiqar, Ghulam Raza, and Nor Aniza Azmi. "Deep learning-based breast cancer classification through medical imaging modalities: state of the art and research challenges." Artificial Intelligence Review 53 (2020): 1655-1720.
39. Nanni, L., S. Brahnam, S. Ghidoni, G. Maguolo, and M. Paci. "General purpose (GenP) bioimage deep ensemble combining new data augmentation techniques and handcrafted features." arXiv (2019).
40. P. L. Stanchev, D. Green, and B. Dimitrov, “High level colour similarity retrieval,” International Journal of Information Theories and Applications, (2003). vol. 10, no. 3, pp. 363-369.
41. Rakshit, Subrata. "New curvelet features for image indexing and retrieval." In Computer Networks and Intelligent Computing: 5th International Conference on Information Processing, ICIP 2011, Bangalore, India, August 5-7, 2011. Proceedings, pp. 492-501. Springer Berlin Heidelberg, 2011.
42. Rana, Shailja, Shruti Jain, and Jitendra Virmani. "SVM-Based Characterization of Focal Kidney Lesions from B-Mode Ultrasound Images." (2016).
43. Rashed, Baidaa Mutasher, and Nirvana Popescu. "Critical Analysis of the Current Medical Image-Based Processing Techniques for Automatic Disease Evaluation: Systematic Literature Review." Sensors 22, no. 18 (2022): 7065.
44. Salau, Ayodeji Olalekan, and Shruti Jain. "Feature extraction: a survey of the types, techniques, applications." 2019 International conference on signal processing and communication (ICSC). IEEE, 2019.
45. Sarwinda, Devvi, Radifa Hilya Paradisa, Alhadi Bustamam, and Pinkie Anggia. "Deep learning in image classification using residual network (ResNet) variants for detection of colorectal cancer." Procedia Computer Science 179 (2021): 423-431.
46. Shaheed, Kashif, Aihua Mao, Imran Qureshi, Munish Kumar, Sumaira Hussain, Inam Ullah, and Xingming Zhang. "DS-CNN: A pre-trained Xception model based on depth-wise separable convolutional neural network for finger vein recognition." Expert Systems with Applications 191 (2022): 116288.
47. Shankar, K., and Eswaran Perumal. "A novel hand-crafted with deep learning features based fusion model for COVID-19 diagnosis and classification using chest X-ray images." Complex & Intelligent Systems 7, no. 3 (2021): 1277-1293.
48. Singh, Vibhav Prakash, and Rajeev Srivastava. "Improved image retrieval using fast Colour-texture features with varying weighted similarity measure and random forests." Multimedia Tools and Applications 77 (2018): 14435-14460.
49. Sultana, Salma, Anik Pramanik, and Md Sadekur Rahman. "Lung Disease Classification Using Deep Learning Models from Chest X-ray Images." In 2023 3rd International Conference on Intelligent Communication and Computational Techniques (ICCT), pp. 1-7. IEEE, 2023.

50. Supriya, S., and M. Subaji. "Intelligent based image enhancement using direct and in-direct contrast enhancement techniques: A comparative survey." International Journal of Signal Processing, Image Processing and Pattern Recognition" 10, no. 7 (2017): 167-184.
51. Sushmithawathi, K., and P. Indra. "Extraction of significant features using GLDM for Covid-19 prediction." Journal of Trends in Computer Science and Smart Technology 3, no. 4 (2022): 287-293.
52. Thanga Selvi, R., and D. Jeyabharathi. "Histogram of Gradients with Deep Features in Coronavirus-19 Diagnosis and Classification Model." In Artificial Intelligence and Evolutionary Computations in Engineering Systems: Computational Algorithm for AI Technology, Proceedings of ICAIECES 2020, pp. 389-399. Springer Singapore, 2022.
53. Van't Hoog, Anna H., Helen K. Meme, Kayla F. Laserson, Janet A. Agaya, Benson G. Muchiri, Willie A. Githui, Lazarus O. Odeny, Barbara J. Marston, and Martien W. Borgdorff. "Screening strategies for tuberculosis prevalence surveys: the value of chest radiography and symptoms." PloS one 7, no. 7 (2012): e38691.
54. Visca, D., C. W. M. Ong, S. Tiberi, R. Centis, L. D'ambrosio, B. Chen, J. Mueller et al. "Tuberculosis and COVID-19 interaction: a review of biological, clinical and public health effects." Pulmonology 27, no. 2 (2021): 151-165.
55. Xu, Yujia, Hak-Keung Lam, and Guangyu Jia. "MANet: A two-stage deep learning method for classification of COVID-19 from Chest X-ray images." Neurocomputing 443 (2021): 96-105.
56. Yue, Jun, Zhenbo Li, Lu Liu, and Zetian Fu. "Content-based image retrieval using color and texture fused features." Mathematical and Computer Modelling 54, no. 3-4 (2011): 1121-1127.
57. Zhang, Jianpeng, Yong Xia, Yutong Xie, Michael Fulham, and David Dagan Feng. "Classification of medical images in the biomedical literature by jointly using deep and handcrafted visual features." IEEE journal of biomedical and health informatics 22, no. 5 (2017): 1521-1530.